Anwendungen

Norman Lang*, Jens Saak, and Peter Benner

Model Order Reduction for Systems with Moving Loads

Modellordnungsreduktion für Systeme mit bewegten Lasttermen

Abstract: In this contribution we present two approaches allowing to find a reduced order approximant of a full order model featuring a moving load term. First, we apply the Balanced Truncation (BT) method to a switched linear system (SLS) using the special structure given in the spatially discretized model. The second approach treats the variability as a continuous parameter dependence and uses the iterative rational Krylov algorithm (IRKA) to compute a parameter preserving reduced order model.

Keywords: Model order reduction, parametric, linear time invariant systems, switched linear systems.

Zusammenfassung: In diesem Beitrag werden zwei Ansätze vorgestellt, welche es erlauben, ein reduziertes Modell eines Originalsystems mit beweglichem Lastterm zu bestimmen. Der erste Ansatz verwendet die Methode des balancierten Abschneidens (BT) zur Reduktion eines geschalteten, linearen Systems (SLS), welches sich aus der speziellen diskreten Struktur des Modells ergibt. Der zweite Ansatz behandelt die Variabilität als eine stetige Parameterabhängigkeit und verwendet den iterativen, rationalen Krylov Algorithmus (IRKA) zur Berechnung eines parametererhaltenden, reduzierten Modells.

Schlüsselwörter: Modellordnungsreduktion, parametrisch, linear zeitinvariante Systeme, geschaltete lineare Systeme.

DOI 10.1515/auto-2014-1095
Received February 18, 2014; accepted May 14, 2014

***Corresponding Author: Norman Lang,** Technische Universität Chemnitz, e-mail: norman.lang@mathematik.tu-chemnitz.de
Jens Saak, Peter Benner: Technische Universität Chemnitz
Jens Saak, Peter Benner: Max Planck Institute for Dynamics of Complex Technical Systems Magdeburg

1 Introduction

Structural variability is a frequently arising problem, for example in machine tool production, due to relatively moving assembly groups. Here, we are investigating one specific occurrence of such variability, namely the problem of moving loads. For demonstration purposes we consider a heat conduction system with relatively moving geometry parts that induce a moving thermal load in one of the subsystems. The two proposed approaches are however applicable to a whole class of systems of this type.

Generating proper reduced order models (ROMs) for the moving load problem is a research topic that gained increasing attention during the recent years. In case of modeling structural variability, which may affect all system matrices, we are actually faced with linear time-varying (LTV) dynamical systems of the form

$$\begin{aligned} E(t)\dot{x}(t) &= A(t)x(t) + B(t)z(t), \\ y(t) &= C(t)x(t). \end{aligned} \tag{1}$$

The matrices $E(t), A(t) \in \mathbb{R}^{n\times n}$ describe the dynamics and $B(t) \in \mathbb{R}^{n\times m}, C(t) \in \mathbb{R}^{q\times n}$ are the input and output matrices, respectively, of the system. Since the dimension n is way too large for many applications, model order reduction (MOR) becomes necessary to keep the computational effort and the storage requirements within numerical algorithms manageable. This is usually an especially demanding task for time-varying systems, when the time dependence of the system matrices is not of very simple structure. An additional issue is to capture the variability as well as stability properties of the original model within the reduced order model. In order to ensure physical interpretability, this task and in particular the special structure of $E(t), A(t), B(t)$ and $C(t)$ will be discussed in the corresponding sections below. We follow two approaches to tackle these difficulties. The first approach is rather pragmatic and exploits the special structure of the spatially discretized system to rewrite it in the form of a switched linear system, where all subsystems are time-invariant. The other

one treats the time dependence as a special incarnation of a parameter dependence. Note that both approaches can be interpreted as discrete approximations of the LTV system. A quantitative investigation of this aspect is, to keep the presentation limited here, postponed to future publications, though.

First, we consider a fixed positioning of the load and therefore end up with a linear time-invariant (LTI) generalized state-space space system of the form

$$\begin{aligned} E\dot{x}(t) &= Ax(t) + Bz(t), \\ y(t) &= Cx(t) \end{aligned} \tag{2}$$

with constant matrices $E, A \in \mathbb{R}^{n\times n}, B \in \mathbb{R}^{n\times m}, C \in \mathbb{R}^{q\times n}$. The goal of MOR now is to compute a ROM of dimension $r \ll n$ of the form

$$\begin{aligned} \hat{E}\dot{\hat{x}}(t) &= \hat{A}\hat{x}(t) + \hat{B}z(t), \\ \hat{y}(t) &= \hat{C}\hat{x}(t) \end{aligned} \tag{3}$$

which satisfies $\hat{y} \approx y$. In case of projection based MOR the reduced order matrices are computed in the form

$$\begin{aligned} \hat{E} &:= W^T EV \in \mathbb{R}^{r\times r}, & \hat{A} &:= W^T AV \in \mathbb{R}^{r\times r}, \\ \hat{B} &:= W^T B \in \mathbb{R}^{r\times m}, & \hat{C} &:= CV \in \mathbb{R}^{q\times r}, \end{aligned}$$

i.e., we need to compute a pair of projection matrices $V, W \in \mathbb{R}^{n\times r}$.

The remainder of this contribution is dedicated to finding and applying those matrices. It is structured as follows. First, we describe the example – a relatively moving machine-stand-slide-structure – which we employ to demonstrate the different model order reduction approaches. This particular example is a system of differential-algebraic equations of index 1 (see Section 2). The MOR approaches which we apply are, however, feasible for all models fitting into this general framework. After introducing the example, we explain a BT based MOR approach for the SLS and a parametric model order reduction (PMOR) scheme based on IRKA. These two approaches are verified by some numerical experiments in Sections 3 and 4. Finally, we give a short summary and an outlook to future developments.

2 The thermo-elastic machine stand model

To illustrate the application of the model reduction methods to be shown, we employ the machine stand example

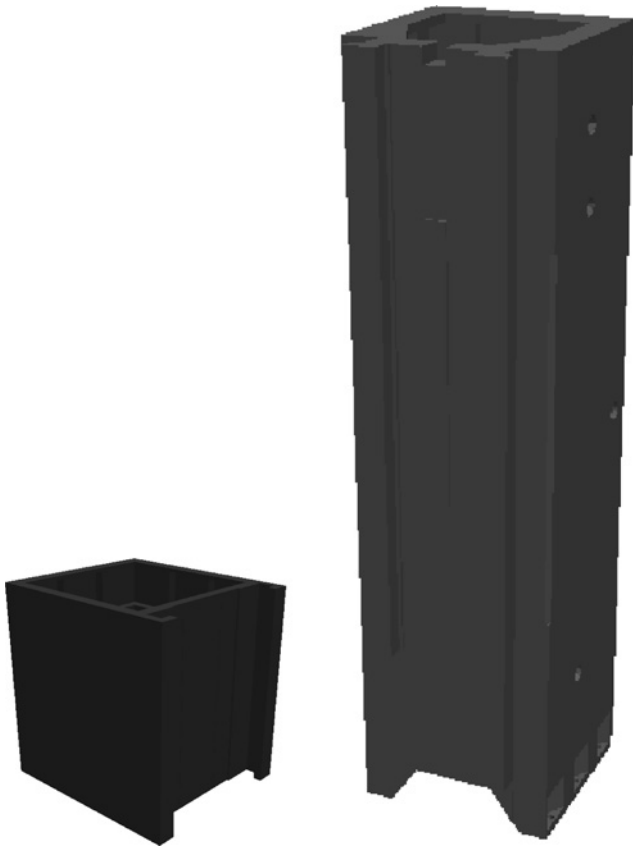

Figure 1: Tool slide and machine stand geometries.

given in [7]. In the example therein, the system variability is induced by a moving tool slide on the guide rails of the stand (see Figure 1). The aim is to determine the thermally driven displacement of the machine stand structure. Following the model setting in [7] the deformation of the stand is assumed to not have any effect on the thermal behavior. This leads to a one-sided coupling of the deformation and heat models. Therefore, we consider the heat equation

$$c_p \rho \dot{T} = \operatorname{div}(\lambda \nabla T), \qquad \text{on } \Omega \tag{4}$$

$$\lambda \frac{\partial}{\partial n} T = q_{fric} + \kappa_c (T_c - T), \qquad \text{on } \Gamma_c \subset \partial\Omega \tag{5}$$

$$\lambda \frac{\partial}{\partial n} T = \kappa_{ext} (T_{ext} - T), \qquad \text{on } \Gamma_{ext} \subset \partial\Omega \tag{6}$$

$$T(0) = T_0, \qquad \text{at } t = 0 \tag{7}$$

where T_c is the temperature of the contact area of the stand and the tool slide, T_{ext} denotes the exterior temperature, c_p is the material specific heat capacity, ρ the density and λ describes the heat conductivity of the stand. The boundary Γ_c denotes the (time) varying contact boundary, which will move with the position of the slide on the stand sur-

face. The equations (5), (6) are third order boundary conditions, i.e., they are so called Robin boundary conditions (see e.g., [17]). According to the boundary parts, Equation (6) describes the heat exchange of the stand with the ambient, whereas Equation (5) models the exchange with the moving slide at the contact boundary Γ_c. In addition to the heat amount exchanged, the latter includes the term q_{fric} induced by friction of the slide movement.

Using a finite element (FE) discretization and denoting the external influences, i.e., the friction driven portion, the heat transferred from the slide at the contact boundary, and the external temperatures, as the system input z, we obtain the dynamical heat model

$$E_{th}\dot{T}(t) = A_{th}(t)T(t) + B_{th}(t)z(t) \tag{8}$$

describing the deformation independent evolution of the temperature field $T \in \mathbb{R}^{n_{th}}$ with the FE mass matrix $E_{th} \in \mathbb{R}^{n_{th}\times n_{th}}$, the varying (with respect to the boundary Γ_c) matrices $A_{th}(t) \in \mathbb{R}^{n_{th}\times n_{th}}$, $B_{th}(t) \in \mathbb{R}^{n_{th}\times m}$ and the thermal input $z \in \mathbb{R}^m$. The particular form of the input z depends on the ansatz we choose and is therefore described in the corresponding sections below. As one can easily check, in this example the variability only affects the system and input matrices $A_{th}(t)$ and $B_{th}(t)$. In order to determine the elastic displacement field of the stand, we additionally need an elasticity model. Since the mechanical behavior of the machine stand is much faster than the propagation of the thermal field, it is sufficient to consider the stationary linear elasticity equations

$$-\operatorname{div}(\sigma(u)) = f, \quad \text{on } \Omega \tag{9a}$$
$$\varepsilon(u) = \mathbf{C}^{-1} : \sigma(u) + \beta(T - T_{ref})I_d, \quad \text{on } \Omega \tag{9b}$$
$$\mathbf{C}^{-1}\sigma(u) = \frac{1+\nu}{E_u}\sigma(u) - \frac{\nu}{E_u}\operatorname{tr}(\sigma(u))I_d, \quad \text{on } \Omega \tag{9c}$$
$$\varepsilon(u) = \frac{1}{2}(\nabla u + \nabla u^T) \quad \text{on } \Omega \tag{9d}$$

to describe the displacement field u. Here, σ denotes the mechanical stress and ε is the strain of the domain Ω. The expression f describes external body forces inducing elastic deformations. In the following example these forces are assumed to be zero. The coefficients E_u, ν, β describe Young's modulus, Poisson's ratio and the thermal expansion coefficient, respectively, depending on the material. The variable $\mathbf{C}$ denotes the stiffness tensor, which is a fourth order tensor and I_d is the identity of dimension d. Here $d = 3$ is the spatial dimension of Ω. For further details on the continuum mechanics related issues in (9) we refer to [5]. The coupling of the thermal and elastic model is given by the expression

$$\beta(T - T_{ref})I_d$$

which describes the thermally driven distortion of the domain Ω. That is, the resulting displacement is induced by the change of temperature T with respect to a given reference temperature T_{ref} of Ω at time t_0. Using the same spatial FE discretization as for the heat model (8), we obtain the algebraic linear system

$$0 = A_{thel}T(t) - A_{el}u(t), \tag{10}$$

where $A_{thel} \in \mathbb{R}^{n_{el}\times n_{th}}$ denotes the coupling of the temperature field T in direction of the displacement field $u \in \mathbb{R}^{n_{el}}$ and $A_{el} \in \mathbb{R}^{n_{el}\times n_{el}}$ is the elasticity system matrix. Since, the influence of the deformation u in direction of the thermal behavior is neglected in the model (4)–(6), there is no coupling matrix $A_{elth} \in \mathbb{R}^{n_{th}\times n_{el}}$. The dimension $n_{el} = 3n_{th}$ denotes the number of elastic degrees of freedom in the FE nodes with respect to the three spatial directions. Assuming the deformation to be small, we consider only translational degrees of freedom as a first test example. Note that the deformation u is not affected by the movement of the tool slide explicitly and therefore the matrices A_{thel}, A_{el} are constant with respect to the structural variability. Introducing $A_{elth} \equiv 0$ due to its absence, we end up with the coupled thermo-elastic system

$$\begin{bmatrix} E_{th} & 0 \\ 0 & 0 \end{bmatrix}\begin{bmatrix} \dot{T} \\ \dot{u} \end{bmatrix} = \begin{bmatrix} -A_{th}(t) & 0 \\ A_{thel} & -A_{el} \end{bmatrix}\begin{bmatrix} T \\ u \end{bmatrix} + \begin{bmatrix} B_{th}(t) \\ 0 \end{bmatrix} z, \tag{11}$$

$$\Leftrightarrow \quad E\dot{x} = A(t)x + B(t)z.$$

Due to the non-singularity of A_{el}, System (11) is a so called index-1 differential algebraic equation (DAE). Since we are interested in the thermally driven deformations at certain points, we consider the output equation

$$y = \begin{bmatrix} 0, & C_{el} \end{bmatrix}\begin{bmatrix} T \\ u \end{bmatrix} = Cx \tag{12}$$

with $C \in \mathbb{R}^{q\times n}$, $n = n_{th} + n_{el} = 4n_{th}$ and $C_{el} \in \mathbb{R}^{q\times n_{el}}$, which only filters the deformation information, we are interested in. In practice, such points might be the tool center point or connections to neighboring assembly groups.

Using an appropriately refined FE discretization, the dimension n of the system becomes very large. Therefore, we apply the BT model order reduction method to an SLS and the IRKA based MOR to a parametric interpretation of the variability in (11), respectively. How to derive the SLS or the parametric system from (11) will be shown in Sections 3 and 4, respectively. Both MOR schemes need to deal with a couple of system solves of dimension n within their procedures. Since n is quite large in many applications, we

aim at full utilization of the special differential-algebraic structure of the coupled thermo-elastic system (11). The application of the Schur complement to Equations (11) and (12) exploits the one-sided coupling, i.e., the zero block in the upper right corner of $A(t)$ (see e.g., [6]) and we obtain

$$\begin{aligned} E_{th}\dot{T} &= A_{th}(t)T + B_{th}(t)z, \\ y &= C_{el}A_{el}^{-1}A_{thel}T = \bar{C}T. \end{aligned} \tag{13}$$

The MOR techniques, we are going to use, now have to be applied to system (13) of dimension n_{th} which is of the same structure as system (11),(12) of dimension n. That is, using the same FE discretization for the thermal and elastic model, we a priori reduce the system dimension from $n = 4n_{th}$ to n_{th}. Again, the particular form of $A(t)$, $B(t)$ or $A_{th}(t)$, $B_{th}(t)$, respectively, will slightly vary with respect to the system interpretation we exploit and therefore will be described in the corresponding sections below.

3 Switched Linear System Approach

The variability of the model is described by time dependent matrices $A_{th}(t)$ and $B_{th}(t)$. This leads directly to the linear time varying system (13). Since model reduction for LTV systems is a highly storage consuming procedure, we exploit properties of the spatially semi-discretized model to set up a switched linear system consisting of LTI subsystems only.

3.1 The switched linear system

Again, following the modelling in [7], the guide rails of the machine stand are modeled as 15 equally distributed horizontal segments (see Figure 2). Any of these segments is assumed to be completely covered by the tool slide if its midpoint (in y-direction) lies within the height of the slide. On the other hand, each segment whose midpoint is not covered is treated as not in contact and therefore the slide always covers exactly 5 segments at each time. This in fact allows the stand to reach 11 distinct, discrete positions given by the model restrictions. These distinguishable setups define the subsystems of the switched linear system

$$\begin{aligned} E_{th}\dot{T} &= A_{th}^{\alpha}T + B_{th}z^{\alpha}, \\ y &= \bar{C}T, \end{aligned} \tag{14}$$

where α is a piecewise constant function of time, which takes its value from the index set $J = \{1, \ldots, 11\}$. That is,

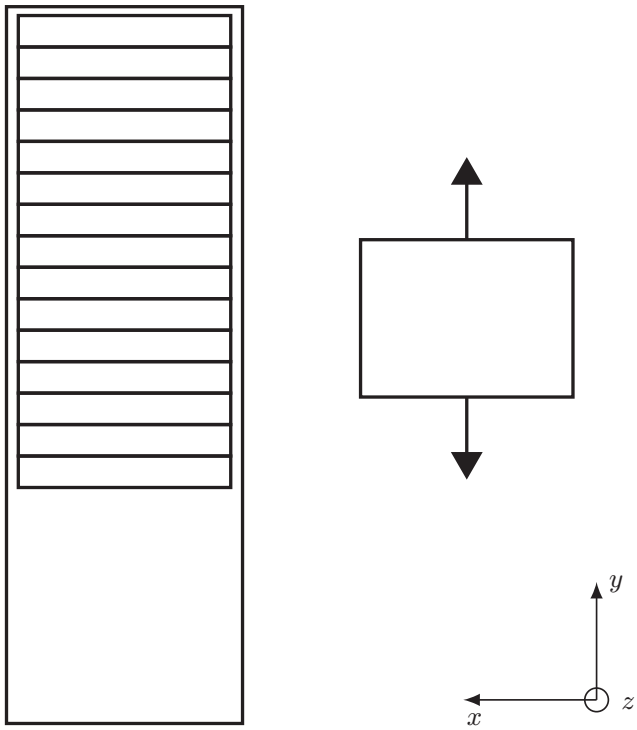

Figure 2: Scheme of partitioned guide rails and moving slide.

$\alpha(t)$ is a time dependent function denoting a switching signal which represents the covered boundary part at time t and thus selects the active subsystem in (14) depending on its value lying in J. Note that the change of the input operator $B_{th}(t)$ is hidden in the input z^{α} itself, since it is sufficient to activate the correct boundary parts by choosing the corresponding columns in B_{th} via the input z^{α}. Therefore, the input operator $B_{th}(t) := B_{th}$ becomes constant and the input variability is represented by the input z^{α}. That is,

$$z_i^{\alpha} := \begin{cases} z_i, & \text{segment } i \text{ is in contact,} \\ 0, & \text{otherwise,} \end{cases} \qquad i = 1, \ldots, 15. \tag{15}$$

Here, $z_i \in \mathbb{R}$ is the thermal input consisting of the friction induced portion q_{fric} and the contact temperature T_c described in Equation (5) and is of the form

$$z_i := q_{fric} + \kappa_c T_c.$$

Here, the actual considered temperature field of the contact surface is approximated by the average of all temperature values in the contact nodes and denoted by T_c. Using the average temperature T_c of the contact area results in equal inputs z_i for all affected segments i for one specific stand-slide configuration. Since the change of the input

domain is described by the input z^α itself, the only varying part influencing the model reduction process left in the dynamical system is the system matrix $A_{th}(t) := A^\alpha_{th}$. In order to find a locally accurate approximate for each of the subsystems $\alpha \in J$, we need to compute individual subspaces V_α, W_α. In order to be able to compute a globally stable reduced order model we need to preserve the stability of each single system and therefore we use the Balanced Truncation method. Note that stability in all subsystems is not sufficient to ensure stability of the entire SLS. For a discussion of stability issues see Section 5.

3.2 BT for switched linear systems

The main ingredient of the BT method is to compute the solutions P_α, Q_α of the controllability and observability Lyapunov equations

$$\begin{aligned} A^\alpha_{th} P_\alpha E^T_{th} + E_{th} P_\alpha {A^\alpha_{th}}^T &= -B_{th} B^T_{th}, \\ {A^\alpha_{th}}^T Q_\alpha E_{th} + E^T_{th} Q_\alpha A^\alpha_{th} &= -\bar{C}^T \bar{C}, \end{aligned} \tag{16}$$

respectively, for each subsystem. Using the Schur complement representation (14) of the coupled thermo-elastic system, the computation of the system Gramians P_α, Q_α is based on the matrices of the thermal model of dimension n_{th} and therefore much cheaper to compute than for the original coupled system of dimension $n = 4n_{th}$. Note that the information of the deformation Equation (10) is completely captured by the modified output matrix $\bar{C}$. The projection matrices are computed by the well known square root method (SRM) (for details on BT see e.g., [4], [11], [14]). Having computed the individual reduced order models, we have to choose the active submodel at each time step via the switching signal $\alpha(t)$ during the simulation.

3.3 Numerical results

For verification we consider a given tool slide trajectory over a time horizon of 16.5 hours. The FE grid consists of 16 626 nodes and at the same time defines the number n_{th} of thermal degrees of freedom. Further, we consider $m = 20$ inputs and therefore $B_{th} \in \mathbb{R}^{n_{th} \times 20}$. The slide temperatures in combination with the friction induced portions acting on the 15 segments on the guide rails (see Equation (15)) are all defined to be separate inputs $z^\alpha_1, \ldots, z^\alpha_{15}$ of the system. Further, we consider constant temperatures at the bottom of the stand and at the left wall (view from behind), respectively, which define the inputs $z^\alpha_{16}, z^\alpha_{17}$. Additionally, we consider the external temperatures T_{ext} in Equation (6) defined by three separated ambient air thresholds in y-direction to be the inputs $z^\alpha_{18}, \ldots, z^\alpha_{20}$. Depending on the switching signal α, the first fifteen inputs vary according to Equation (15). In order to evaluate the forward simulation of the model and to compare the reduced and full order SLS, respectively, we define nine nodes for observation on the surface of the stand. Three of them are located at each of the side walls and another three at the guide rails. Since the deformations in the spatial directions are considered in each observation node, we end up with $q = 27$ outputs. Note that for performing the forward simulation of the reduced order model we need to switch between the individual subspaces V_α, W_α since the reduced states

$$\hat{x}_\alpha = (W^T_\alpha E_{th} V_\alpha)^{-1} W^T_\alpha E_{th} x$$

reside in different subspaces. The expression $W^T_\alpha E_{th} V_\alpha$ is built to be the identity of dimension r within the BT method and therefore we have to apply a projection

$$\hat{x}_{\alpha^+}(t^+_s) = W^T_{\alpha^+} E_{th} V_{\alpha^-} \hat{x}_{\alpha^-}(t^-_s) \tag{17}$$

at every switching time t_s.

The projection describes the reset of the reduced state vector $\hat{x}$ with respect to the switching from subspaces $V_{\alpha^-}, W_{\alpha^-}$ to $V_{\alpha^+}, W_{\alpha^+}$ at switching time t_S. In order to avoid the computation of the reduced state transformation $W^T_{\alpha^+} E_{th} V_{\alpha^-}$ at every switching instance, the products should be precomputed. This leads to an increasing offline phase and storage amount but fastens the online phase significantly. Figure 3 shows the full order time domain evolution of one of the deformation nodes at the guide rails of the stand compared to the trajectories of reduced order models of dimension 10, 40 and 60, respectively. Note that the subsystems in all possible stand-slide configurations α are computed to be of the same size. Since we have

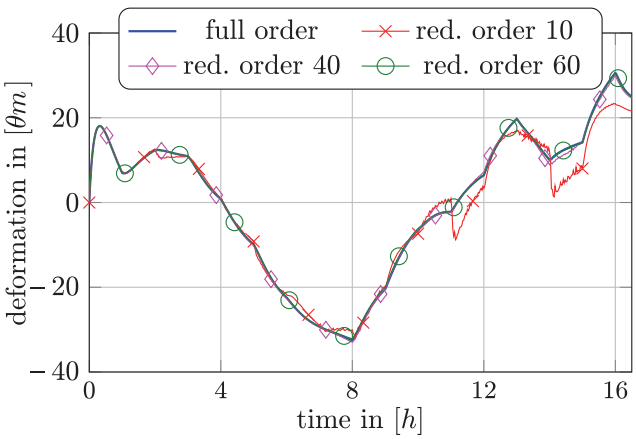

Figure 3: Displacement evolution of the full order system compared to ROMs of order $r = 10, 40$ and 60.

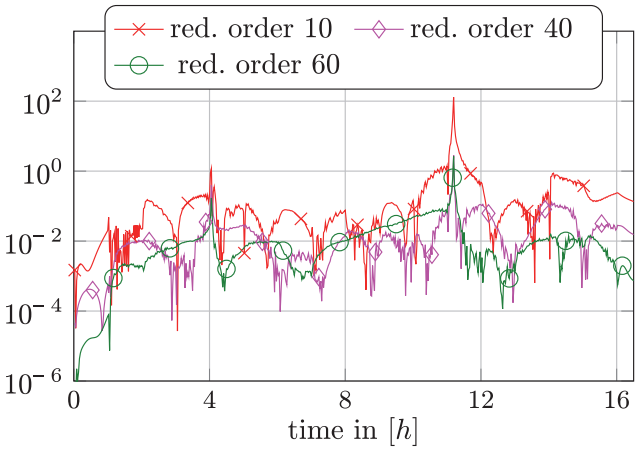

Figure 4: Relative error of reduced order models of order $r = 10, 40$ and 60 in time domain.

to switch between the individual subspaces V_α, W_α anyway, this is not required to achieve compatibility for the different subsystems with respect to the switching. Nevertheless, the equality of reduced dimensions will be of particular importance for stability reasons as we will see in Section 5. In Figure 4, the relative error of the full order model and the reduced order models is depicted. The results show that a reduced order of 60 allows the reproduction of the full order trajectory with an average error in the per mill range. The peaks in Figure 4, showing a relative error larger than 10^{-1}, are caused by the division by a number close to zero related to the zero crossings of the deformation trajectory (see Figure 3) and are therefore showing up for numerical reasons only.

4 Parametric System Approach

Noting that the computation of a reduced order model for each subsystem of the SLS and the state-space transformations in each switching step in the previous section are quite expensive, in this section we consider the structural variability to be a continuous parameter $\mu(t)$. In the future we also want to investigate techniques as e.g., matrix interpolation as proposed in [1, 15] in order to avoid the state transformations in every switching instance of the SLS approach.

4.1 The parametric system

The varying position of the tool slide serves as the parameter dependence of the system. Depending on $\mu(t)$, the active boundary parts Γ_c in Equation (5) are determined and the Schur complement representation (13) becomes the generalized parametric state-space system

$$\begin{aligned} E_{th}\dot{T} &= A_{th}(\mu)T + B_{th}(\mu)z, \\ y &= \bar{C}T \end{aligned} \tag{18}$$

with $A_{th}(t) := A_{th}(\mu(t))$ and $B_{th}(t) := B_{th}(\mu(t))$. The goal here is to find a global ROM with respect to the parameter μ in such a way that the physical interpretability of the parameter is preserved.

4.2 IRKA for parametric systems

Following the theory in [2], we use the iterative rational Krylov algorithm (IRKA) to compute $\mathcal{H}_2$ optimal ROMs via the projection matrices

$$\begin{aligned} V_j &:= \left[\ldots, \quad (\sigma_\ell E - A_{th}(\mu_j))^{-1} B_{th}(\mu_j) b_\ell, \quad \ldots\right], \\ W_j &:= \left[\ldots, \quad (\sigma_\ell E - A_{th}(\mu_j))^{-T} \bar{C}^T c_\ell, \quad \ldots\right]. \end{aligned} \tag{19}$$

The projection bases V_j, W_j describe the input and output Krylov subspaces of the system (18) in the parameter sample point μ_j. Here σ_ℓ denotes the frequency interpolation points and b_ℓ, c_ℓ the tangential interpolation directions for all $\ell = 1, \ldots, r_j$ (for details on IRKA see, e.g. [2, 9]). The pairs V_j, W_j with $j = 1, \ldots, k$ in selected parameter sample points $\mu_1, \ldots, \mu_k$ are combined by concatenation to generate a pair of global projection matrices

$$V = \left[V_1, \ldots, V_k\right], \quad W = \left[W_1, \ldots, W_k\right] \in \mathbb{R}^{n_{th} \times r}$$

with $r = \sum_{j=1}^{k} r_j$. It should be mentioned that the resulting matrices V, W in general do not generate a globally $\mathcal{H}_2$ optimal reduced order model although each of the subsystems fulfills the optimality conditions at μ_j. Using these projection bases to compute a set of reduced order matrices of the form

$$\hat{A}_{th}(\mu) = W^T A_{th}(\mu) V, \quad \hat{B}_{th}(\mu) = W^T B_{th}(\mu)$$

for each parameter value μ during the online simulation of the system is a highly time consuming procedure. Therefore, we consider an efficient splitting of the computations into an offline and online part. That is, the parameter dependence of the system matrices $A_{th}(\mu), B_{th}(\mu)$ is rewritten in an affine form

$$\begin{aligned} A(\mu) &= A_0 + f_1(\mu)A_1 + \cdots + f_{m_A}(\mu)A_{m_A}, \\ B(\mu) &= B_0 + g_1(\mu)B_1 + \cdots + g_{m_B}(\mu)B_{m_B}, \end{aligned} \tag{20}$$

where $m_A, m_B \in \mathbb{N}$. Note that the numbers of summands m_A and m_B does not necessarily have to be equal. Such

a parameter affine representation can always be achieved, see e.g., [10]. Given this form, the parameter dependent matrices $A(\mu), B(\mu)$ can be reduced in the form

$$\hat{A}(\mu) = \sum_{i}^{m_A} f_i(\mu) W^T A_i V, \qquad \hat{B}(\mu) = \sum_{i}^{m_B} g_i(\mu) W^T B_i, \tag{21}$$

where the computation of $W^T A_i V, W^T B_i$ is parameter independent and therefore performed in the offline stage. Using the affine representation (20), the structure of the parameter dependence is automatically preserved and the online evaluation of the parameter is reduced to the evaluation of the functions $f_i, g_i, i = 1, \ldots, m_A/m_B$. These functions may be linear or non-linear, but are assumed to be smooth enough to allow for interpolation.

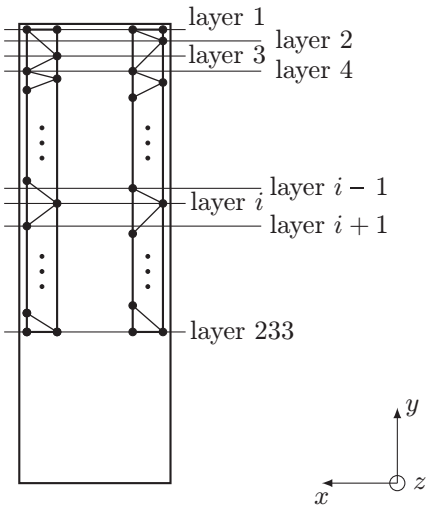

Figure 5: Parameter affine splitting based on horizontal layers with same y-coordinates of FE nodes.

4.3 Numerical results

Considering the example described in Section 3.3, we have to compute an affine representation for the parameter dependent matrices $A_{th}(\mu)$ and $B_{th}(\mu)$ first. In contrast to the partition of the guide rails into 15 segments given by the model description [7], here we consider the parameter dependence to be continuous, and therefore discard the segmentation given in the SLS approach. We decompose the guide rails as fine as possible in order to get a nearly continuous representation of the movement. In case of the machine stand simulation example, the affine parameter representation of the matrices $A_{th}(\mu)$ and $B_{th}(\mu)$ is based on a horizontal splitting of all FE nodes on the guide rails which have the same vertical coordinate. That means, we split the matrices into a sum of m_A/m_B submatrices $A_i, B_i, i = 1, \ldots, m_A/m_B$, each consisting of all nodes corresponding to one specific horizontal layer. The functions f_i, g_i in Equation (20) are equal and of the form

$$f_i(\mu) = \begin{cases} 1, & \text{the } i\text{-th horizontal layer is in contact,} \\ 0, & \text{otherwise.} \end{cases}$$

That is, the functions $f_i(\mu), g_i(\mu)$ activate the parts of Γ_c, which are covered by the tool slide, depending on the position μ. The given FE grid and the corresponding discretization lead to a splitting of the guide rails into 233 disjoint horizontal layers (see Figure 5). In fact, $m_A = m_B = 233$ depend on the resolution of the FE grid at the guide rails, i.e., a grid refinement will immediately lead to increasing numbers m_A, m_B. In terms of the online computation time, the affine representation, is most advantageous for $m_A, m_B \ll n_{th}$, since the number of function evaluations with respect to the parameter μ will increase proportionally with the number of summands m_A, m_B. On the other hand, in terms of the overall computation time, the splitting (20) and the associated precomputation of the reduced matrices in (21) will pay off for a large number of parameter evaluations, e.g., in case of parameter studies. Due to the parameter affine splitting and the associated summation of the matrix summands A_i, B_i related to the active boundary layers, the corresponding inputs $z_1^\alpha, \ldots, z_{15}^\alpha$ reduce to a single input. That is, in the parametric model we deal with $m = 6$ inputs instead of 20 inputs as in the SLS. Again, input z_1 describes the temperature input of the tool slide combined with the friction induced portion in Equation (15) and $z_2, \ldots, z_6$ are equal to the inputs $z_{16}^\alpha, \ldots, z_{20}^\alpha$ of the SLS.

For reasons of stability of the global reduced order model, here we use a one-sided projection framework (for details see Section 5). One has to decide for either using V or W. The most obvious idea here is to choose W. That is, considering the Schur complement, the deformation information, which is completely encoded in the basis W (see Equation (19)) of the output Krylov space via the output matrix

$$\bar{C} := C_{el} A_{el}^{-1} A_{thel}$$

is kept while generating the global ROM. Nevertheless, the following figures show that for the machine stand example both implementations of the one-sided Galerkin projection lead to pretty similar results. These results are based on the choice of $k = 3$ parameter sample points, equally distributed over the parameter range starting in the inter-

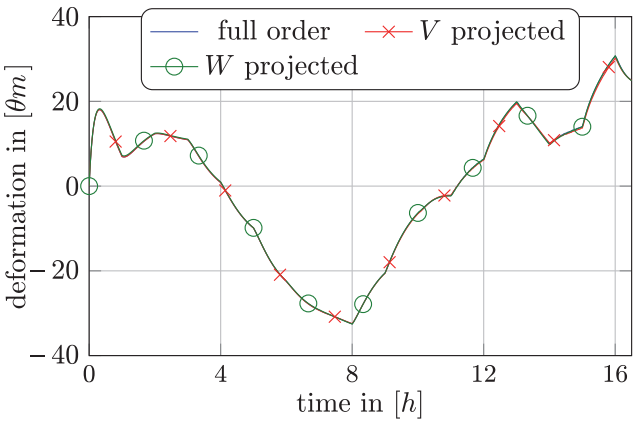

Figure 6: Displacement evolution of the full order system compared to the ROM of order $r = 75$ generated by input (V) or output (W) Krylov subspaces, respectively.

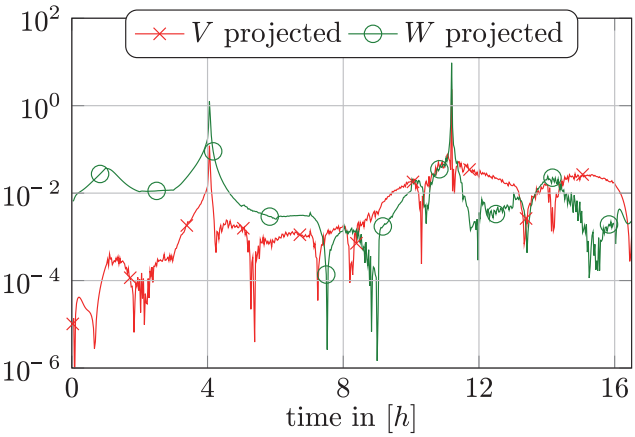

Figure 7: Relative error of the reduced order models of order $r = 75$ in time domain.

val bounds. The matrices V_j, W_j are of size $r_j = 25$, $\forall j = 1, \ldots, k$. This leads to global reduced order models of size $r = 75$. The full order deformation trajectory compared to the reduced order models generated by either the one-sided projection via V or W, respectively, are depicted in Figure 6. Both ROMs produce relative errors in the per mill range as presented in Figure 7. Here again, the relative errors with largest magnitude are related to the zero crossings of the deformation trajectory at $t \approx 4[h]$ and $t \approx 11[h]$. Further, we observe that the ROM based on the one-sided V-projection comes up with slightly better results in the first half of the simulation, whereas the W-projection leads to the better results in the second half. Some reasons will be discussed in the following Section 5.

5 Discussion

In this section the advantages and disadvantages of the shown model order reduction approaches, as well as some basics on stability observations will be discussed and summarized.

5.1 Comparison of the results

As the Figures 3, 4, 6 and 7 show, both MOR approaches lead to nearly the same accuracy, but the IRKA based PMOR method needs significantly less time. An overview of the system orders, the offline reduction timings and simulation times is given in Table 1. In case of the machine stand example, using the PMOR scheme, it is sufficient to compute local reduction bases in $k = 3$ parameter sample points μ_k which results in k runs of IRKA. On the other hand in case of the SLS we apply the BT method to each of the 11 subsystems which is observable in the offline reduction times. Considering the online timings the SLS approach based on BT leads to a significant faster online simulation for the full and reduced order systems. This is due to the fact that for the SLS scheme we have exactly 11 possible stand-slide configurations and additionally the heat model is solved for a fixed time-step size. That means, the solution operator of the linear subsystems associated to α does not change in every time step and therefore we can recycle the corresponding solvers for the linear subsystems. In case of the parametric model the variability described by the parameter μ is considered to be continuous and therefore there is no fixed number of discrete positions as in the SLS case. That means, since the operator of the linear system changes continuously, we cannot recycle the solvers for the linear systems in a comparable simple way. Finally, with respect to the timings, the parametric approach achieves significant better results in the offline phase while the SLS ansatz results in better online timings. Nevertheless, there are other properties of the methods which should be taken into account.

Table 1: Comparison of system orders, times for the reduction processes and the corresponding simulation times for the full and the reduced order systems for the SLS approach and the PMOR scheme, respectively.

	sys. order	red. time	sim. time
full order SLS	16 626	–	43.11 [s]
reduced SLS	60	4560.32	0.69 [s]
full order PAR	16 626	–	1028.22 [s]
reduced PAR	75	2090.56	1.76 [s]

5.2 BT for SLS

As mentioned in Section 3, the BT method was applied in order to preserve the stability of the subsystems of the SLS. But in general, stability of the subsystems does not guarantee stability of the SLS. It is well-known (see e.g. [12]) that an SLS (14) is exponentially stable if all subsystems share a common quadratic Lyapunov function (CQLF)

$$\mathcal{L}(x) = x^T \mathcal{P} x, \tag{22}$$

where $\mathcal{P}$ is the symmetric positive definite (spd) solution of the linear matrix inequality

$$A_{th}^{\alpha} \mathcal{P} + \mathcal{P} A_{th}^{\alpha\ T} \leq -\mathcal{S} \tag{23}$$

for some spd matrix $\mathcal{S}$. Furthermore, it is not guaranteed that the reduced SLS is stable if the full order SLS shares a CQLF and the stability of the subsystems is preserved by e.g., using BT. The reduced order SLS also needs to fulfill the condition of sharing a CQLF. Since in this case we compute individual projection bases V_α, W_α, the reduced systems in general evolve in different subspaces. If this is the case, the reduced subsystems can not share a CQLF. Then, it becomes necessary to fulfill additional conditions. For example, find a set of state space transformations L_α^{-1} which projects all subsystems into the same subspace and at the same time ensure that a CQLF is shared (see [8]). Another way is to follow the idea of simultaneous balancing as proposed in [13]. Therein, a pair of global projection matrices V, W as in the parametric case is computed in order to capture the most important states of all of the subsystems. Note that the machine stand example described in this contribution does not require any of the additional considerations since the reduced order model, based on the stable subsystems generated by BT, appeared to result in a stable SLS of reduced order as the numerical results in Section 3.3 show. Another very important property is that the well known error bound

$$\|G(.) - \hat{G}(.)\|_{\mathcal{H}_\infty} \leq 2 \sum_{\ell=r+1}^{n} \sigma_\ell,$$

with the transfer functions of the full and reduced order model $G, \hat{G}$, respectively, and the Hankel singular values σ_ℓ, of the Balanced Truncation method for LTI systems can be extended to the SLSs [16].

5.3 PMOR via IRKA

In case of the machine stand example shown in the previous sections, the parametric model reduction approach yields very good results. But still there is no guarantee for stability of the reduced order model even if the single ROMs in the sample points μ_k are stable. As mentioned in the corresponding section, we have implemented a one-sided Galerkin projection with $V = W$, which ensures stability of the ROM, instead of the usual Petrov-Galerkin projection. Another issue which should be taken into account is the parameter affine representation (20) of the parametric matrices. Since it is not unique and the number of summands in there directly influences the computational effort it is recommended to keep the number of summands as small as possible. Furthermore, not having given such an affine representation it becomes necessary to find an appropriate approximation to obtain the affine form (20). Still, in our experience this introduces another approximation error. Finally, compared to the BT method the PMOR scheme does not provide an error bound yet. Note that it is also well known that the convergence behavior within IRKA becomes worse for an increasing predefined reduced order r.

5.4 PMOR via BT and IRKA for SLS

Note that the BT method can be used in the PMOR case, as well as the IRKA for the SLS. But still, using BT within the described PMOR procedure, in general one would lose the balancing property of the local reduction bases V_k, W_k with respect to parameter sample points μ_k for the resulting global ROM during the concatenation step and therefore lose the theoretical background of BT, that is, e.g. the error bound. Another approach using BT and interpolation for parametric model reduction is described in [3]. The application of IRKA to the SLS in general would lead to unstable subsystems. Thus, ensuring stability the usage of a one-sided projection in each single subsystem becomes necessary. This might lead to additional errors with respect to the accuracy and therefore generate additional instability problems regarding the global ROM. Therefore, the stability preservation and the existence of an error bound for the quality of the ROM make the BT method the better choice for the SLS approach.

6 Conclusion and Outlook

We have seen that both the Balanced Truncation method applied to a switched linear system interpretation, as well as an interpolatory projection method for a parametric model interpretation based on the iterative rational Krylov algorithm can achieve relative MOR errors in the per mill

range for moderate reduced orders. Thereby, the comparison is performed with respect to the full order discretized model. Although, both approaches neglect the LTV nature of the physical model to some extent, assuming that the full order model is a sufficient approximation to the physical LTV system, the additional error resulting from the MOR should be negligible.

In the future we will address the quantification of the approximation error with respect to the physical model, as well as we investigate efficient strategies to deal with model order reduction for linear time varying systems. In particular the BT method for LTV models will lead to the solution of differential Lyapunov equations, where it is still an open question how to solve these differential matrix equations and especially store their solutions efficiently.

Acknowledgement: This research was funded by the Deutsche Forschungsgemeinschaft DFG as subproject A06 *"Model Order Reduction for Thermo-Elastic Assembly Group Models"* of the Collaborative Research Center/Transregio 96 *"Thermo-energetic design of machine tools – A systemic approach to solve the conflict between power efficiency, accuracy and productivity demonstrated at the example of machining production"*. At this point we thank subproject A05 *"Simulation of active machine tool models"* for providing the spatial FE-discretizations of the machine stand and slide geometries used as the demonstration example throughout this article.

References

1. D. Amsallem and C. Farhat, An online method for interpolating linear parametric reduced-order models, *SIAM J. Sci. Comp., 33 (2011), pp. 2169–2198*.
2. U. Baur, C. A. Beattie, P. Benner, and S. Gugercin, Interpolatory projection methods for parameterized model reduction, *SIAM J. Sci. Comput., 33 (2011), pp. 2489–2518*.
3. U. Baur and P. Benner, Modellreduktion für parametrisierte Systeme durch balanciertes Abschneiden und Interpolation (Model Reduction for Parametric Systems Using Balanced Truncation and Interpolation), *at-Automatisierungstechnik, 57 (2009), pp. 411–420*.
4. D. F. Enns, Model reduction with balanced realizations: An error bound and a frequency weighted generalization, *The 23rd IEEE Conference on Decision and Control, 23 (1984), pp. 127–132*.
5. M. R. Eslami, R. B. Hetnarski, J. Ignaczak, N. Noda, N. Sumi, and Y. Tanigawa, Theory of Elasticity and Thermal Stresses, *Springer-Verlag, Dordrecht, 2013*.
6. F. Freitas, J. Rommes, and N. Martins, Gramian based reduction method applied to large sparse power system descriptor models, *IEEE Trans. Power Systems, 23 (2008), pp. 1258–1270*.
7. A. Galant, K. GroÃ§mann, and A. Mühl: Model Order Reduction (MOR) for Thermo-Elastic Models of Frame Structural Components on Machine Tools. *ANSYS Conference & 29th CADFEM UsersâĂŹ Meeting 2011, October 19-21, 2011, Stuttgart, Germany*.
8. M. Geuss and K. J. Diepold, An approach for stability-preserving model order reduction for switched linear systems based on individual subspaces, *in Methoden und Anwendungen der Regelungstechnik, Günter Roppenecker and Boris Lohmann, eds., Shaker Verlag, Aachen, Sep. 2013*.
9. S. Gugercin, A. C. Antoulas, and C. Beattie, $\mathcal{H}_2$ model reduction for large-scale dynamical systems, *SIAM J. Matrix Anal. Appl., 30 (2008), pp. 609–638*.
10. B. Haasdonk and M. Ohlberger, Efficient reduced models for parametrized dynamical systems by offline/online decomposition, *in Proc. MATHMOD 2009, 6th Vienna International Conference on Mathematical Modelling, 2009*.
11. A. J. Laub, M. T. Heath, C. C. Paige, and R. C. Ward, Computation of system balancing transformations and other applications of simultaneous diagonalization algorithms, *IEEE Trans. Automat. Control, 32 (1987), pp. 115–122*.
12. D. Liberzon, Switching in Systems and Control, *Springer-Verlag, New York, 2003*.
13. N. Monshizadeh, H. L. Trentelman, and M. K. Camlibel, Simultaneous balancing and model reduction of switched linear systems, *in The 50th IEEE Conference on Decision and Control and European Control Conference, IEEE, 2011, pp. 6552–6557*.
14. B. C. Moore, Principal component analysis in linear systems: controllability, observability, and model reduction, *IEEE Trans. Automat. Control, AC-26 (1981), pp. 17–32*.
15. H. Panzer, J. Mohring, R. Eid and B. Lohmann, Parametric Model Order Reduction by Matrix Interpolation *at-Automatisierungstechnik, 58 (2010), pp. 475-484*.
16. M. Petreczky, R. Wisniewski, and J. Leth, Balanced truncation for linear switched systems, *Nonlinear Analysis: Hybrid Systems, 10 (2013), pp. 4-20*.
17. W. A. Strauss, Partial Differential Equations: An Introduction, *Whiley & Sons, Ltd.,Hoboken, US, 2008*.

Dipl.-Math. techn. Norman Lang
Technische Universität Chemnitz, Fakultät für Mathematik, Mathematik in Industrie und Technik, Reichenhainerstr 39/41, D-09126 Chemnitz
norman.lang@mathematik.tu-chemnitz.de

Dipl.-Math. techn. Norman Lang is a research assistant at the Fakultät für Mathematik at the Technische Universität Chemnitz. His research interests include optimal control with applications on inverse problems, (parameter preserving) model order reduction and the solution of large-scale matrix equations (in particular the differential Riccati and Lyapunov equations).

Dr. Jens Saak
Max Planck Institute Magdeburg, Computational Methods in Systems and Control Theory, Sandtorstr 1, D-39106 Magdeburg

Dr. Jens Saak is a postdoctoral researcher in the Computational Methods in Systems and Control group at the Max Planck Institute for Dynamics of Complex Technical Systems in Magdeburg. His fields of research include the solution of large-scale and sparse matrix equations, model order reduction, the investigation of numerical methods in optimal control of partial differential equations, as well as, the scientific and high performance computing aspects of the above.

Prof. Dr. Peter Benner
Max Planck Institute Magdeburg, Computational Methods in Systems and Control Theory, Sandtorstr. 1, D-39106 Magdeburg

Prof. Dr. Peter Benner is one of the directors and head of the Computational Methods in Systems and Control group at the Max Planck Institute for Dynamics of Complex Technical Systems in Magdeburg. His research activities include numerical linear algebra, model reduction and systems approximation, parallel algorithms, linear quadratic optimization, robust stabilization of linear and non-linear systems and control of instationary PDEs.